3D Beamforming for Spectral Coexistence of Satellite and Terrestrial Networks

Shree Krishna Sharma*, Symeon Chatzinotas*, Joel Grotz†, Björn Ottersten*
*SnT - securityandtrust.lu, University of Luxembourg, Luxembourg
Email: {shree.sharma, symeon.chatzinotas, bjorn.ottersten}@uni.lu
†Technical Labs, Newtec, Belgium, Email: joel.grotz@newtec.eu

***Abstract*—Satellite communication (SatCom) is facing a spectrum scarcity problem due to the limited available exclusive spectrum and the high demand of the broadband satellite services. In this context, there has been an increasing interest in the satellite community to exploit the non-exclusive Ka-band spectrum in order to enhance the spectral efficiency of future broadband satellite systems. Herein, we propose a novel concept of enabling the spectral coexistence of satellite and terrestrial networks using three dimensional (3D) beamforming, which exploits the elevation dimension in addition to the commonly used azimuth dimension. The proposed beamforming solution is employed in a Multiple-Input Low Noise Block Downconverter (MLNB) based Feed Array Reflector (FAR) in contrast to the widely used Uniform Linear Array (ULA) structure. Within the employed antenna structure, the performance of the proposed beamforming solution is evaluated considering different feed arrangements. Finally, a database-assisted approach and two blind approaches are suggested for the effective implementation of the proposed solutions.**

I. Introduction

Next generation Satellite Communication (SatCom) systems are targeting higher throughput and enhanced spectral efficiency in order to meet the increased consumer broadband demand over satellites. Although a significant number of high throughput Ka-band multibeam satellite systems have been already deployed, there is still a large gap with respect to the spectral efficiency requirement of the next generation Terabit/s satellites within the 2020 horizon [1]. One of the main bottlenecks in meeting this requirement is the limitation in the available Ka-band exclusive spectrum (only 500 MHz in the uplink and the same in the downlink) [2]. In this context, the exploitation of the non-exclusive band can be one of the promising solutions to enhance the spectral efficiency of future SatCom systems.

As in terrestrial wireless systems, the concept of cognitive coexistence is receiving increasing attention lately in the satellite research community, referred to as cognitive SatComs [2], [3]. The existing literature can be broadly categorized into [4]: (i) hybrid satellite-terrestrial coexistence, and (ii) dual satellite coexistence [5]. The first category deals with the spectral coexistence of satellite and terrestrial networks over the same spectrum whereas the latter deals with the spectral coexistence of two satellite networks. Out of these, this paper focuses on the first scenario.

Beamforming (BF) has been considered as one of the important enabling techniques for Cognitive Radio (CR) communications due to its spatial filtering capability. The main difference between a conventional BF problem and the cognitive BF problem is the introduction of interference constraints imposed by the incumbent system while designing a beamformer. Recently, cognitive BF approaches have been widely studied for different secondary network optimization objectives such as sum rate maximization, power minimization with Quality of Service (QoS) constraints, and rate balancing (see [6] and references therein). However, in the context of cognitive SatComs, only a few works exist in the literature [7]–[9].

Motivation and Contributions: Most of the existing BF schemes control the radiation pattern in the azimuthal plane. This category of BF can be referred as two dimensional (2D) BF. Its main drawback is that it does not consider elevation dimension in designing the beamformer and hence the beampattern is not adapted in the elevation plane. To overcome this drawback, the concept of 3D BF has recently received important attention in terrestrial wireless literature [10]–[13]. In contrast to 2D BF, the 3D BF controls the radiation beam pattern in both elevation and azimuth planes, thus providing additional degrees of freedom (dofs) in the elevation plane while designing a wireless system. In terrestrial cellular systems, the 3D BF approach can provide several benefits such as less intercell and intersector interference, higher system throughput, better energy efficiency, improved coverage extension, and the increased spectral efficiency, and thus has been considered as a candidate technique for the fifth generation (5G) of wireless systems [10].

Despite increasing research interest towards 3D BF in the terrestrial paradigm [10]–[13], the application of 3D BF to the satellite-terrestrial coexistence scenario is a novel and interesting research problem. This is the main focus of this paper. In SatCom systems, elevation angle of a satellite terminal may vary over a large geographical region and it provides an additional dof for enabling the spectral coexistence scenarios. In this paper, we investigate the application of 3D BF approach for the spectral coexistence of Geostationary (GEO) Fixed Satellite Services (FSS) and terrestrial Fixed Service (FS) microwave links. The terrestrial FS links are highly directive in the Earth's horizontal plane whereas FSS terminals are directive towards the GEO satellite. In this context, an FSS terminal may employ 3D BF in order to minimize interference towards the plane in which FS interference is concentrated and to maximize its transmission towards the desired direction. In contrast to the conventional 2D approach, we exploit the additional dof provided by the elevation dimension in order to design a 3D beamformer at the FSS terminal for enabling the spectral coexistence of GEO satellite and terrestrial microwave links, which is a novel application field.

In most of the existing adaptive BF works, linear and planar arrays, i.e., Direct Reflecting Arrays (DRA) are used for 2D BF and 3D BF cases, respectively. However, in SatCom applications, the most dominant antenna structure is the offset parabolic reflector due to its high gain. In this context, the focus of this paper is on the BF design using a feed array based offset reflector. The designed beamformer benefits from both the high gain of the reflector as well as the spatial filtering capability of the feed array. The concept of using an array feed, especially the cluster feeds in a parabolic reflector has been used for several applications such as generation of multiple beams, generation of contour beams, for improving the scanned performance, and for directivity optimization (see [14] and references therein), etc. However, the existing works on the use of an array feed for adaptive array processing are limited and they mainly focus on the satellite/gateway side rather than the terminal side. In the context of terminal-side beamforming, the authors in [15] used this antenna structure for mitigating the adjacent satellite interference. In this paper, we are motivated by a cost effective design compatible with consumer grade products and therefore choose the array fed reflector design for employing 3D BF at the FSS terminal.

Organization: The remainder of this paper is organized as follows: Section II describes the considered scenario and highlights the underlying problems to be addressed. Section III presents the signal model. Section IV proposes the BF design framework considering both antenna structure and the BF weight design while Section V highlights the implementation aspects. Section VI evaluates the performance of the proposed BF solutions with the help of numerical results. Finally, Section VII concludes the paper.

II. Scenario and Problem Description

We consider the spectral coexistence of a GEO FSS satellite downlink and a terrestrial FS link both operating in the Ka-band ($17.7-19.7$ GHz) as depicted in Fig. 1. In this scenario, the FS link and FSS satellite downlink are incumbent (primary) and cognitive (secondary) links, respectively. There may occur interference from the FSS satellite to the FS receivers and from the FS transmitting stations to the FSS terminals. The downlink interference from the cognitive satellite to the FS links is usually taken into account by system planning and can be kept below the defined regulatory limitations in terms of the maximum power flux-density (pfd) at the Earth's surface [16]. Therefore, the interference from the FSS satellite to the FS receivers can be considered to be negligible in practice. However, the interference from FS transmitters to the FSS terminal needs to be managed properly in order to guarantee the desired rate of the cognitive users.

In order to address the aforementioned issue, we propose to apply 3D BF at the FSS terminal equipped with a Multiple-Input Low Noise Block Downconverter (MLNB) based Feed Array Reflector (FAR) utilizing the elevation dimension. GEO FSS terminals have special directive characteristics that they always look into the GEO satellite with a fixed elevation angle with respect to a satellite. This specific feature has been exploited in our previous works [7], [8] while designing

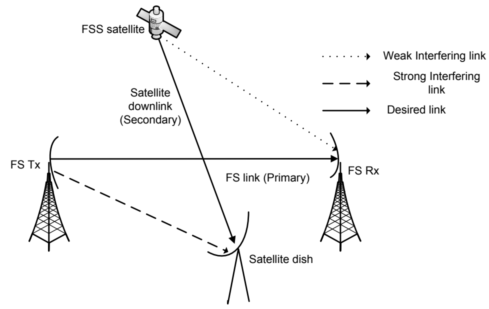

Fig. 1. Spectral coexistence of FSS downlink with the microwave FS link in $17.7-19.7$ GHz

different transmit and receive BF techniques at the base station of a terrestrial wireless system in order to enable the spectral coexistence of C-band satellite system and terrestrial cellular systems. Furthermore, in the considered scenario, FS transmissions are also highly directive in the Earth's horizontal plane and these two different types of directive features motivate us to exploit 3D BF in the considered scenario.

Moreover, another research issue in the considered FAR structure is to find a suitable feed configuration which satisfies the desired BF performance criteria. Different feed configurations may provide different beamforming patterns which may affect the desired performance criteria. In this context, we also evaluate beamforming performance considering different feed configurations.

III. Signal Model

In this paper, we consider a narrowband signal model for the BF design. We assume that the FSS terminal is equipped with an MLNB based FAR consisting of M number of multiple LNBs. Let (ϕ_0, θ_0) denote the 2D angular position of the desired satellite and (ϕ_j, θ_j), $j \in \{j = 1, ..., J\}$, denotes the 2D location of the jth interfering user with J being the number of interfering FS stations. Then the $M \times 1$ received signal vector $\mathbf{y}$ at the FSS terminal can be written as

$$\mathbf{y} = h_0 \mathbf{a}(\phi_0, \theta_0) s_0 + \sum_{j=1}^{J} h_j \mathbf{a}(\phi_j, \theta_j) s_j + \mathbf{z}, \qquad (1)$$

where s_0 is the desired transmitted signal, s_j is the transmitted signal from the jth interfering FS transmitter, $\mathbf{z}$ denotes the $M \times 1$ Additive White Gaussian Noise (AWGN) vector, $\mathbf{a}(\phi_0, \theta_0)$ denotes the antenna response vector for the impinging plane wave coming from the direction (ϕ_0, θ_0), $\mathbf{a}(\phi_j, \theta_j)$ denotes the antenna response vector towards the jth interfering FS station, h_j represents the channel gain for the jth user and it is assumed to be constant for all feeds in the array. The response vector $\mathbf{a}(\phi, \theta)$ for the considered FAR antenna is given by

$$\mathbf{a}(\phi, \theta) = [g_1 e^{j\Psi_1}, g_2 e^{j\Psi_2}, \ldots, g_M e^{j\Psi_M}]^T, \qquad (2)$$

where g_i and Ψ_i denote the amplitude gain and the phase of the ith feed ($i = 1, \ldots, M$) to a unit amplitude plane wave coming from the direction (ϕ, θ), respectively.

At the output of the beamformer, the received signal vector $\mathbf{y}$ in (1) is linearly combined through an $M \times 1$ complex weight vector $\mathbf{w}$ to yield the output y_1 in the following way

$$y_1 = \mathbf{w}^\dagger \mathbf{y}, \qquad (3)$$

TABLE I. FEED POSITIONS FOR DIFFERENT CONFIGURATIONS

First Case (3 LNBs)		Second Case (7 LNBs)
Configuration 1 (see Fig. 2(a))	Feed 1: x=0,y=0,z=0.45 Feed 2: x=0.0169, y=0, z=0.45 Feed 3: x=0.0338, y=0, z=0.45	Configuration 4 (see Fig. 3.) Feed 1: x=0,y=0,z=0.45 m
Configuration 2 (see Fig. 2(b))	Feed 1: x=0,y=0,z=0.4331 Feed 2: x=0, y=0, z=0.45 Feed 3: x=0, y=0, z=0.4669	Feed 2: x=-0.0084, y=0.0146, z=0.45 Feed 3: x=-0.0169, y=0, z=0.45 Feed 4: x=-0.0084, y=-0.0146, z=0.45
Configuration 3 (see Fig. 2(c))	Feed 1: x=0,y=0.0084, z=0.45 Feed 2: x=-0.0084, y=-0.0146, z=0.45 Feed 3: x=0.0084, y=-0.0146, z=0.45	Feed 5: x=0.0084, y=-0.0146, z=0.45 Feed 6: x=0.0169, y=0, z=0.45 Feed 7: x=0.0084, y=0.0146, z=0.45

where $(\cdot)^\dagger$ denotes the Hermitian transpose. The employed BF design is detailed in the following section.

IV. BEAMFORMER DESIGN

The two main aspects which characterize the performance of a beamformer are [9]: (i) antenna structure, and (ii) design of BF weights, which are desribed in the following subsections.

A. Antenna Structure and Feed Geometry

As mentioned before, we consider an offset parabolic reflector with an array feed. The aperture diameter of the reflector is considered to be 0.75 m and the ratio of the focal length to the aperture diameter f/D is considered to be 0.6, which is typical for a consumer reflector antenna. The assumed feed geometry is a typical MLNB setup with 3 to 7 feeds with different arrangements. To have the better BF performance, the feed arrangement can be optimized jointly being able to receive the desired satellite signal with the sufficient gain and to mitigate the harmful interference coming from the FS transmitters based on the interference threshold constraint.

The main difference in the BF design while employing the widely used ULA structure and the considered FAR structure lies in the array response vector i.e., $\mathbf{a}(\phi,\theta)$ in (2). The array response vector for the ULA is analytically derivable using the knowledge of the wavelength of the impinging plane wave λ and the antenna spacing d in the array whereas no analytical derivation is available for the FAR and it must be calculated numerically. In the considered MLNB-based FAR, the response vector for each individual feed while including the effect of the reflector is calculated using the software GRASP, which is based on well-established reflector antenna analysis techniques [17].

We base our BF evaluation on a cost effective consumer product design approach and intend to keep the number of array elements small. The feed positions (all distances in m) presented in Table I are considered as the practical feed positions on the antenna. In the first case, we consider the FAR with 3 LNBs, and in order to investigate the additional benefit of more array elements, we consider 7 LNBs in the second case. In all the configurations, the distance between two feeds is considered to be equal to the wavelength λ.

B. Beamforming Techniques

The existing BF solutions can be broadly categorized into [18]: (i) statistically optimum, and (ii) deterministic. For the considered scenario in this paper, we propose the 3D form of the Linearly Constrained Minimum Variance (LCMV) beamformer, which falls under the first category.

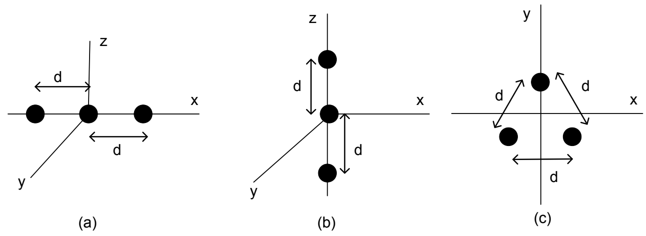

Fig. 2. Considered feed arrangements with 3 array elements in the MLNB (a) horizontal (Configuration 1), (b) vertical (Configuration 2), (c) triangular in the xy plane with $z = 0.45$ (Configuration 3). The center of the coordinate system in above configurations correspond to (x=0, y=0, z=0.45 m).

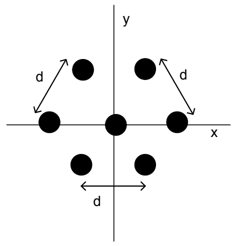

Fig. 3. Hexagonal feed geometry with 7 LNBs in the xy plane (Configuration 4)

1) LCMV Technique: In this beamformer, the BF weights are designed to minimize the output variance or power subject to multiple response constraints. Unlike the Minimum Variance Distortionless Response (MVDR) or Capon beamformer, the standard LCMV beamformer includes multiple response constraints with a unity response in the desired direction and null responses in the interfering directions. The optimization problem for the standard LCMV beamformer can be written as

$$\begin{aligned} &\min_{\mathbf{w}} \mathbf{w}^\dagger \mathbf{R}_y \mathbf{w} \\ \text{subject to } &\mathbf{w}^\dagger \mathbf{a}(\phi_d,\theta_d) = 1 \\ &\mathbf{C}^\dagger \mathbf{w} = \mathbf{f}, \end{aligned} \tag{4}$$

where $\mathbf{C}$ is an $M \times J$ constraint matrix, $\mathbf{f}$ is an $J \times 1$ response vector, $\mathbf{R}_y$ is the sample covariance matrix of the received signal, given by; $\mathbf{R}_y = \frac{1}{N}\sum_{i=1}^{N} \mathbf{y}(n)\mathbf{y}^H(n)$, with N being the number of samples. For the application in our scenario, we propose the following two modifications of the LCMV beamformer.

1. Proposed 3D LCMV Method 1: In this case, we modify the standard LCMV beamformer in the 3D form. The response towards all the interfering directions is considered to be null. In this case, the second constraint in (4) can be rewritten as

$$\begin{bmatrix} \mathbf{a}^\dagger(\phi_1,\theta_1) \\ \mathbf{a}^\dagger(\phi_2,\theta_2) \\ \vdots \\ \mathbf{a}^\dagger(\phi_J,\theta_J) \end{bmatrix} \mathbf{w} = \begin{bmatrix} \sqrt{G_{\max}} \\ 0 \\ \vdots \\ 0 \end{bmatrix}. \tag{5}$$

where $G_{\max}$ is the desired maximum gain towards the intended satellite. The solution of the problem (4) with the second constraint from (5) becomes same as the solution of the standard LCMV, given by [19]

$$\mathbf{w} = \mathbf{R}_y^{-1}\mathbf{C}(\mathbf{C}^\dagger \mathbf{R}_y^{-1}\mathbf{C})^{-1}\mathbf{f}. \tag{6}$$

2. Proposed 3D LCMV Method 2: The response towards the interfering directions is considered to be some small value ϵ rather than zero. In this case, the second constraint in (4) can be written as

$$\mathbf{C}^{\dagger}\mathbf{w} = \mathbf{f}_1, \tag{7}$$

where $\mathbf{f}_1 = [\sqrt{G_{\max}}, \epsilon, ..., \epsilon]$. Then the solution for the BF weight is given by (6), with $\mathbf{f}$ replaced by $\mathbf{f}_1$.

V. Implementation Aspects

In the considered antenna structure, a designer may have the flexibility of placing the feed elements somewhat arbitrarily and hence the element patterns usually become different. For employing the 3D BF algorithms described in Section IV-B, we need the Direction of Arrivals (DoAs) of the incoming signals from the desired satellite and from the FS stations. The DoA of the signal from the desired satellite is usually known based on the desired FSS satellite location but the DoAs of the interfering signals have to be obtained by some mechanisms such as DoA estimation or database [9]. Since the interfering signals from the FS stations may come from anywhere in the azimuthal plane containing the Earth's local horizon, ideally it would be effective to mitigate interference coming from the whole horizon. However, this may not be feasible due to the limited dofs available at the FSS terminal to create the desired pattern. In this context, we suggest the following applicable approaches.

1. Database-assisted approach: In this approach, the DoAs of the interfering signals are assumed to be known with the help of the database [9]. This database can be constructed either with the help of available information from regulators/operators or with the help of sensing measurements. In practice, the number of MLNBs should be kept as low as possible due to cost and implementation issues [15]. Thus in practice, in case multiple interfering FS stations are present, 2 or 3 significant number of interfering FS terminals need to be taken into account.

2. Blind approach: In case the database is not available, BF can be implemented based on the awareness of the interfering/victim sector [7], [8]. For selecting the interfering sector, we propose the following two approaches

i. The main lobe of the FSS terminal is usually expected to receive the higher level of the interference from the FS transmitters. Thus, the azimuthal sector which contains the main lobe can be considered as the interfering sector. Since the half power beamwidth of a typical FSS terminal antenna (with an aperture diameter of 0.75 m) operating at the frequency of 17.7 GHz is $1.5773°$, by considering an azimuthal sector of more than $3.14°$, we can ensure the effective mitigation of the FS interference which may enter into the main lobe of the antenna.

ii. Since GEO satellite terminals have special properties that they look into the fixed GEO satellite (towards south if we consider the Northern hemisphere), they receive interference form a specific sector [7], [8]. In this context, with the help of the link analysis of the GEO satellite, the interfering sector from where the harmful interference may come to the terminal can be determined. For the considered FSS-FS coexistence scenario, it's usually the Earth's horizontal plane in the southern side of the FSS terminal.

TABLE II. Simulation Parameters

Parameter	Value/Type
Carrier frequency	17.7 GHz
Aperture diameter (D)	0.75 m
Focal length (f)	0.45 m
f/D	0.6
Taper angle	$37.75°$
Taper	-12 dB
Polarization	Linear
Feed clearance	0.075 m
Number of LNBs	3,7
Distance between feeds	0.0169 m
$G_{\max}$	41.67 dBi
Terminal location	$49.6833°$ N, $6.35°$ E
GEO Sat. location	$28.2°$ E

VI. Numerical Results

For evaluating the performance of the considered feed configurations, first, we generate antenna patterns using the GRASP tool [17] and then apply the designed BF weights. The main simulation parameters are provided in Table II.

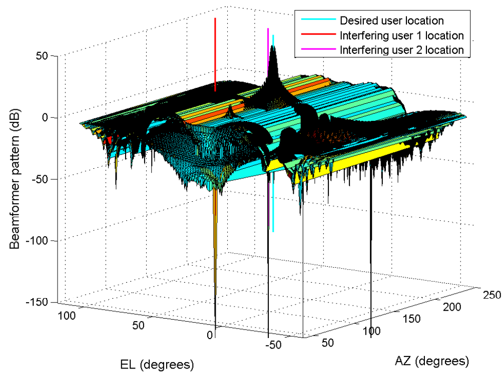

Fig. 4. Response pattern of the 3D LCMV beamformer with feed configuration 1, $\epsilon = 0$, desired satellite location: (elevation $= 29.3°$, azimuth $= 152.2°$), Interfering user 1 location: (elevation $= 85.88°$, azimuth $= 176.97°$, Interfering user 2 location: (elevation $= 41.92°$, azimuth $= 167.68°$

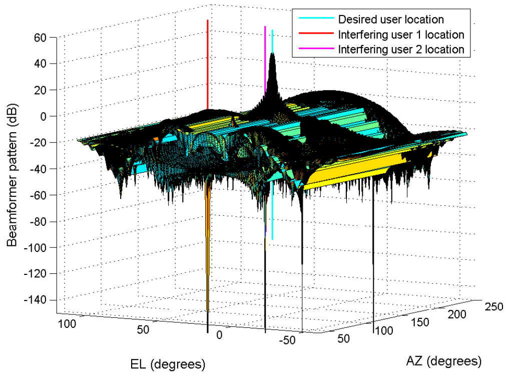

Fig. 5. Response pattern of the 3D LCMV beamformer with feed configuration 2, $\epsilon = 0$

Figures 4, 5 and 6 depict the response patterns of the proposed 3D LCMV with feed configurations 1, 2 and 3, respectively considering $\epsilon = 0$. It can be depicted that in configurations 1 and 2, the beamformer produces the response of 41.67 dB in the desired direction and less than -200 dB in the interfering directions. One main difference of these patterns from the pattern with the configuration 3 in Fig. 6 is that grating nulls are observed in Figs. 4 and 5, which is

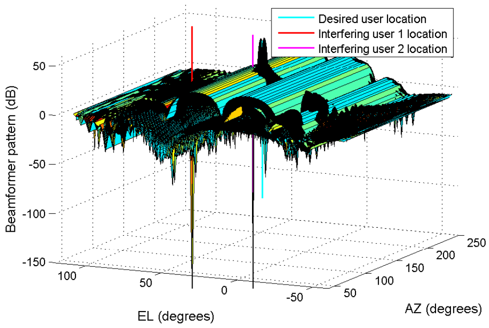

Fig. 6. Response pattern of the 3D LCMV beamformer with feed configuration 3, $\epsilon = 0$

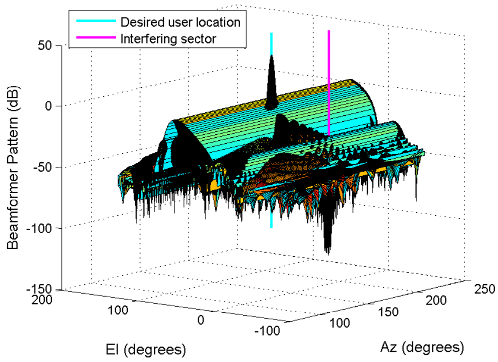

Fig. 7. Response pattern of the 3D LCMV beamformer with feed configuration 4, $\epsilon = 10^{-6}$

not the case in Fig. 6. Avoiding grating nulls leads to a better Signal to Interference plus Noise Ratio (SINR) performance since the output SINR from the beamformer gets decreased if the desired DoA lies near to the grating null [20]. The grating nulls can be avoided either by choosing the proper array element patterns or by choosing a suitable feed geometry as illustrated in this paper. Furthermore, another observed difference is that the beamfomer's gain in the main lobe of the configuration 3 is higher than in other configurations. From the above observations, it can be concluded that BF pattern of the considered antenna structure depends on the chosen feed configuration.

Furthermore, from the simulation study, it has been noted that the configurations with 3 MLNBs is capable of producing nulls only in two main interfering directions (not presented here due to space limitations). Thus, we have to use higher number of LNBs if the number of the significant interfering FS stations exceeds 2. In Fig. 7, we present the response pattern for configuration 3 with 7 MLNBs arranged in a hexagonal configuration with $\epsilon = 10^{-6}$. For this result, we consider the sector mitigation based on the second blind approach presented in Section V. We assume that the interfering sector is known but the specific interfering directions within the sector are unknown. From the result, we can see that the considered 3D LCMV approach with the hexagonal feed configuration can effectively mitigate interference from the interfering sector of more than 5° azimuthal span.

VII. Conclusions

This paper has proposed a novel concept of using 3D beamforming for enabling the spectral coexistence of GEO FSS satellite with the FS microwave links utilizing the MLNB based FAR instead of the commonly used ULA antenna structure. The response patterns of different feed configurations have been compared with the help of realistic antenna patterns obtained from the GRASP tool. It has been observed that the BF pattern is dependent on the configuration of the array feed geometry. Furthermore, it has been shown that the hexagonal feed configuration with 7 LNBs can effectively mitigate interference coming from the interference sector with more than 5° azimuthal span. In our future work, we plan to study the iterative adaptation between BF weight design and feed configurations as well as the design of robust 3D BF approaches.

Acknowledgement

This work was supported by FNR, Luxembourg under the CORE projects “SeMIGod” and “SATSENT”.

References

[1] O. Vidal *et al.*, “Next generation high throughput satellite system,” in *IEEE First ESTEL*, Oct. 2012, pp. 1–7.

[2] K. Liolis *et al.*, “Cognitive radio scenarios for satellite communications: The CoRaSat approach,” in *FUNMS*, July 2013, pp. 1–10.

[3] S. K. Sharma, S. Chatzinotas, and B. Ottersten, “Satellite cognitive communications: Interference modeling and techniques selection,” in *6th ASMS and 12th SPSC*, Sept. 2012, pp. 111–118.

[4] S. K. Sharma, S. Chatzinotas, and B. Ottersten, “Cognitive radio techniques for satellite communication systems,” in *IEEE 78th VTC Fall*, Sept. 2013, pp. 1–5.

[5] S. K. Sharma, S. Chatzinotas, and B. Ottersten, “In-line interference mitigation techniques for spectral coexistence of GEO and NGEO satellites,” *Int. J. Satellite Commun. and Networking*, Sep. 2014.

[6] G. Zheng, K.-K. Wong, and B. Ottersten, “Robust cognitive beamforming with bounded channel uncertainties,” *IEEE Trans. Signal Process.*, vol. 57, no. 12, pp. 4871–4881, Dec. 2009.

[7] S. K. Sharma, S. Chatzinotas, and B. Ottersten, “Transmit beamforming for spectral coexistence of satellite and terrestrial networks,” in *8th Int. Conf. CROWNCOM*, July 2013, pp. 275–281.

[8] S. K. Sharma, S. Chatzinotas, and B. Ottersten, “Spatial filtering for underlay cognitive SatComs,” in *PSATS Conf.*, vol. 123, pp. 186–198.

[9] S. K. Sharma *et al.*, “Joint carrier allocation and beamforming for cognitive SatComs in Ka-band (17.3-18.1 GHz),” in *Proc. IEEE ICC*, June 2015.

[10] S. Mohammad Razavizadeh, M. Ahn, and I. Lee, “Three-dimensional beamforming: A new enabling technology for 5G wireless networks,” *IEEE Signal Process, Mag.*, vol. 31, no. 6, pp. 94–101, Nov. 2014.

[11] W. Lee *et al.*, “Downlink vertical beamforming designs for active antenna systems,” *IEEE Trans. Commun.*, vol. 62, no. 6, pp. 1897–1907, June 2014.

[12] J. Xu and J. Zhang, “An attempt to 3D capon beamforming,” in *8th Int. Conf. CHINACOM*, Aug. 2013, pp. 734–739.

[13] H. Halbauer *et al.*, “3D beamforming: Performance improvement for cellular networks,” *Bell Labs Technical J.*, no. 2, pp. 37–56, Sept. 2013.

[14] J. Duggan and P. McLane, “Adaptive beamforming with a multiple beam antenna,” in *IEEE ICC*, vol. 1, June 1998, pp. 395–401.

[15] J. Grotz, B. Ottersten, and J. Krause, “Signal detection and synchronization for interference overloaded satellite broadcast reception,” *IEEE Trans. Wireless Commun.*, vol. 9, no. 10, pp. 3052–3063, Oct. 2010.

[16] ITU, “Radio Regulations”, ITU-R, Article 21, 2004.

[17] GRASP, http://www.ticra.com/products/software/grasp, 2000.

[18] B. Van Veen and K. Buckley, “Beamforming: a versatile approach to spatial filtering,” *IEEE ASSP Mag.*, vol. 5, no. 2, pp. 4 –24, Apr. 1988.

[19] R. Lorenz and S. Boyd, “Robust minimum variance beamforming,” *IEEE Trans. Signal Process.*, vol. 53, no. 5, May 2005.

[20] A. Ishide and R. T. Compton, “On grating nulls in adaptive arrays,” *IEEE Trans. Antennas and Propag.*, vol. 28, no. 4, July 1980.